

## PDMS Nanoslits without Roof Collapse

Jinyong Lee, Young-Keu Yun, Yoori Kim, and Kyubong Jo\*

*Department of Chemistry and Interdisciplinary Program of Integrated Biotechnology, Sogang University, Seoul 121-742, Korea. \*E-mail: jokyubong@sogang.ac.kr*

*Received June 10, 2009, Accepted June 29, 2009*

Soft lithography of polydimethyl-siloxane (PDMS), an elastomeric polymer, has enabled rapid and inexpensive fabrications of microfluidic devices for various biochemical and bioanalytical applications. However, fabrications of nanostructured PDMS components such as nanoslits remain extremely challenging because of deformation of PDMS material. One of the well-known issues is the unwanted contact between the surfaces of PDMS roof and bottom substrate, called 'roof collapse'. Here we have developed a novel approach for the facile stabilization of PDMS nanoslits in the low height (130 nm)/width (100  $\mu\text{m}$ ) ratio without roof-collapse. Within 130 nm high nanoslits, we demonstrate the confinement of single DNA molecules. We believe that this approach will serve as a key to utilize PDMS as nanoslits for integrated microfluidic devices.

**Key Words:** Nanoslit, Roof collapse, Flexibility, Surface hydration, Confinement

### Introduction

Micro- and nanofabricated devices have recently provided unprecedented routes for biochemical and bioanalytical systems, such as DNA chips, biosensors, microreactors, micro- or nano-electromechanical systems (MEMS, NEMS), and micro total analytical systems (TAS).<sup>1-5</sup> For these various applications, soft lithography has emerged as an alternative to conventional photolithography and electron-beam lithography. Soft lithography is a suite of techniques that uses organic materials to enable replication and pattern transfer on multiple length scales from nanometers to centimeters, developed as a method of reproducing numerous patterns by replica molding from the same master.<sup>6,7</sup> The characteristics of soft lithography are advantageous for biological applications because of simplicity, low cost, rapid prototyping, compatibility with cells and ease of use. Also, polydimethyl-siloxane (PDMS) – the most commonly used material in soft lithography – has several attractive characteristics: It is soft, transparent, permeable to gases, impermeable to water, biocompatible and has a low electrical conductivity. Another important property of PDMS is the structural flexibility that is advantageous in most applications, but flexible structures often cause problems in nanostructure applications because of difficulty in maintaining nanometer scale structures without deformation.

Although a number of previous studies have used PDMS for sub-micron nanostructures,<sup>8,9</sup> most of nano-devices for manipulating single molecules such as DNA or proteins have been developed by using hard materials such as quartz or fused-silica.<sup>10-12</sup> Nevertheless, nanofabrication of hard materials is still technologically demanding and time-consuming with the need for expensive lithographic equipment for each device. After fabrication, patterned nanofluidic devices require enclosure such as anodic or fusion bonding, but these sealing processes are relatively complicated and make nanodevices unusable after one time use. While silicon wafer is being utilized in conventional nanotechnology, the semiconductor attributes of silicon wafers lead most researchers to use

insulatory quartz or fused-silica for such fabrications because electrokinetic control is very common for biomolecule manipulation in miniaturized devices. Toilsome fabrication of each device and the expense of quartz or fused-silica materials necessitate their reuse which leads to contamination problems. Therefore, hard materials are not appropriate ones to produce a large number of disposable devices for high-throughput bioanalytical applications.<sup>7,13</sup> To overcome the limitations of hard materials, disposable PDMS devices are ideal for high-throughput bioanalytical applications.

Among various functional nanofluidic structures, nanoslits are useful for manipulating single molecules due to distinct advantages nanoslits have: First, molecules can be simultaneously monitored on optical or fluorescent microscopes because all molecules are in the same focal depth; the focal depth of optical or fluorescent microscope with high magnification (e.g. 100  $\times$  objective lens) is usually less than 500 nm. In the typical microfluidic devices, some molecules are in focus but many other molecules are out of focus resulting in blurred complicated images to interpret. Second, flow rates and diffusions in nanoslits are extremely slow because of high fluidic resistance of nanostructures. This property allows us to control nanofluid with electrophoretic force in more sophisticated manners without fluidic disturbance. Third, the nanoslit can mimic two-dimensional system for the investigation of molecular behaviors. In particular, single DNA molecules' conformations and diffusions in nanoslits have been intensively investigated in nanoslits for the understanding of two-dimensional behavior of DNA polymer chains.<sup>14,15</sup>

Previously PDMS nanoslits of 100 nm  $\times$  1  $\mu\text{m}$  has been implemented for genomic analysis of single DNA molecules, but the width of 1  $\mu\text{m}$  is too small to show two dimensional characteristics.<sup>8</sup> Except these 1  $\mu\text{m}$  wide narrow nanoslits, other nanoslit applications have been limited to the fabrication based on hard materials such as quartz or fused-silica each nanoslits device should be fabricated *via* technologically demanding nanofabrication process.<sup>14-16</sup> Thus, if structurally stable PDMS nanoslits are readily available, nanoslits will be

more broadly utilized for various biochemical and bioanalytical applications. In addition, this availability of PDMS nanoslits will help non-fabrication experts such as chemists or biologists perform bioanalytical applications using nanoslits because replica molding of PDMS nanoslits are much easier to follow than technologically demanding nanofabrication of hard materials. Nonetheless, PDMS nanoslits have not been available due to constraints coming from structural deformation. One of the well-known PDMS deformation issues is the roof collapse, contact between the surfaces of the PDMS roof and the bottom substrate. The characteristics of roof collapse have been theoretically and experimentally investigated by several groups who are interested in micro contact printing using PDMS stamps.<sup>17-20</sup>

Here we demonstrate a novel approach to make PDMS nanoslits without roof-collapse. For this development, we have tested various widths and heights. Also, we have changed factors possibly increasing the stability of PDMS nanoslits such as changing the surface hydrophilic; restraining the device deformability; pre-filling the gap of PDMS nanoslits and glass substrate with water. The combination of these three approaches leads to stabilize 130 nm high and 100  $\mu\text{m}$  wide PDMS nanoslits. Within 130 nm nanoslit, we demonstrate the conformation of DNA molecules more widely stretched than ones within 1  $\mu\text{m}$  high microslit.

### Experimental Section

**Reagents.** Photoresist SU-8 2005, thinner SU-8 2000 and SU-8 developer (MicroChem) were obtained from K1 Solution (Seoul, Korea). AZ-GXR601 and AZ1500 thinner were obtained from Hyodong Chemical Engineering (Incheon, Korea). Glass coverslips (24  $\times$  60 mm No. 1 thickness) were obtained from Daihan Scientific (Seoul, Korea). Stock of YOYO-1 in DMSO (dimethyl sulfoxide) was purchased from Invitrogen (Pure Bio, Seoul, Korea). T4 DNA (166 kbps, 0.52  $\mu\text{g}/\mu\text{L}$ ) were purchased from Nippon Gene (Eugentech Inc, Daejeon, Korea). Polydimethyl-siloxane (Sylgard 184, PDMS) was purchased from Sewang Hightech (Seoul, Korea). Tridecafluoro-1,1,2,2-tetrahydro octyl-trichloro silane were purchased from United Chemicals (Good Science, Daejeon, Korea).

**Fabrication of PDMS Nanoslit.** Fabrication of PDMS devices followed standard rapid prototyping procedures.<sup>7,13,21</sup> Slit patterns were drawn in AutoCAD 2007. The widths of slits were 20  $\mu\text{m}$ , 40  $\mu\text{m}$ , 60  $\mu\text{m}$ , 80  $\mu\text{m}$ , and 100  $\mu\text{m}$ . The Cr mask and wafers with different heights were fabricated in Amed Inc (Seoul, Korea). The heights were controlled by mixing ratio between positive photoresist AZ-GXR 601 and ZA1500 thinner, resulting in 130 nm, 230 nm, 340 nm, 490 nm, and 1330 nm, respectively. 2150 nm high pattern was fabricated by using SU-8 2002. The heights were measured by alpha-step profilometer. Vapor deposition of tridecafluoro-1,1,2,2-tetrahydro octyl-trichloro silane was used for silanization of the patterned wafer to promote PDMS releasing.<sup>13,21</sup> The PDMS pre-polymer mixed with curing agent (10:1 weight ratio) was cast on the patterned wafer and cured at 65  $^{\circ}\text{C}$  for 12 h or longer, which is longer than typical PDMS curing time in order to make PDMS nanodevices more rigid. Cured PDMS

was peeled off from the patterned wafer and then PDMS devices were treated in an air plasma generator for 30 s (Femto Science Cute Basic, Hwaseong, Korea) to make PDMS surface hydrophilic. Right after plasma treatment, a PDMS device can strongly adhere on the glass surface; sometimes a PDMS device is irreversibly bonded to the glass.<sup>21</sup> This irreversible covalent bonding is critically problematic when a PDMS roof collapses on the glass substrate. In order to avoid this irreversible bonding capability, we have stored PDMS devices in water for at least a couple of minutes since we have observed that plasma treated PDMS device stored in water do not irreversibly adhere on the glass substrate. Also, water storage preserves the hydrophilicity of PDMS surface longer than several days.<sup>22</sup>

#### PDMS Nanoslit Mounting on Glass without Roof Collapse.

In order to prevent roof collapse, PDMS nanoslit was mounted on a bent glass substrate. For bending the glass substrate, both ends of a frame (75 mm  $\times$  25 mm  $\times$  2 mm made of acrylic resin) on which a coverslip was attached were inwardly pushed. While the cover glass was slightly being bent, a PDMS nanoslit device was mounted on the bent cover glass. This method allowed some space between PDMS nanoslits and the cover glass for water to fill. After filling water in this gap, the force exert on the plastic frame was removed, resulting in the formation of stable nanoslits.

**DNA Sample Preparation and Loading.** DNA samples were prepared containing T4 DNA (0.01  $\mu\text{g}$ ) with YOYO-1 (0.25  $\mu\text{M}$ ), Tris EDTA buffer (pH 8.0, 0.03  $\times$  TE 300  $\mu\text{M}$  Tris and  $\mu\text{M}$  EDTA), 4%-mercaptoethanol (v/v, HSCH<sub>2</sub>CH<sub>2</sub>OH). The stock solution of T4 DNA has 0.5 mg/mL concentration. This stock solution was diluted to 50 times in 1  $\times$  TE buffer (10 mM Tris and 1 mM EDTA) before experiment. To make the DNA sample, 3  $\mu\text{L}$  of T4 DNA solution (1/50 of stock solution) was diluted with 91  $\mu\text{L}$  water and 2  $\mu\text{L}$  YOYO-1 (0.25 mM) and 4  $\mu\text{L}$   $\beta$ -mercaptoethanol to final volume of 100  $\mu\text{L}$  since the low ionic condition promotes DNA stretching in nanoslits. DNA solution was mounted on the entrance of nanoslits which was previously filled with water. Then, on the other exit side of nanoslits we applied gentle negative pressure for suction to drive DNA solution into nanoslits.

**Microscopy and Image Processing.** Microscopy system consisted of an inverted microscope (Zeiss Observer A1, Hyun Bio, Seoul, Korea) equipped with a 63  $\times$  Zeiss Plan-Neofluar oil immersion objective illuminated by a solid state laser (Coherent Sapphire 488, Wooyang, Seoul, Korea). A holographic notch filter for 488 nm (Nam Il Optical Components Corp, Incheon, Korea) was installed to prevent 488 laser light from reaching CCD camera. Fluorescence images were captured by a charge-coupled device digital camera (CCD, Roper Scientific CoolSNAP EZ, 1392  $\times$  1040 pixels, 12-bit digitization) and stored as 16 bit TIFF format generated by a software of RS Image (Roper Scientific, ASK, Seoul, Korea)

### Results and Discussion

**Roof Collapse.** Roof collapse is a well-known phenomenon that PDMS nanoslits of large width and nanometer scale height collapse and disappear as illustrated in Fig. 1. A conceivable hypothesis to explain this phenomenon is that

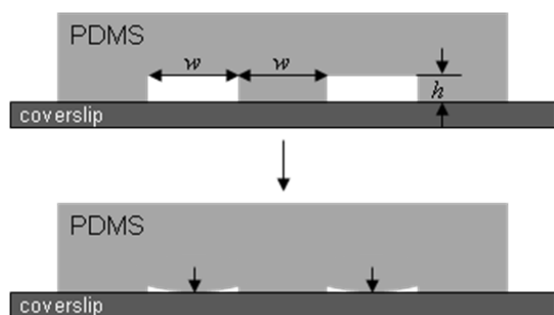


**Figure 1.** Roof collapse of PDMS nanoslits. Nanoslit pattern has height of  $h$ , and the same length of width and spacing of  $w$ . High aspect ratio of width to height leads to roof collapse of PDMS device. Especially, the roof collapse is a serious issue if the height ( $h$ ) is less than a micrometer and the width is pretty wide. Here the width of nanoslit is set to the same length of spacing to simplify the relationship of a theoretical model (Eqs. 1 and 2).

gravitational sagging may cause roof collapse due to self-weight of PDMS device.<sup>17,23</sup> However, some experimental observations are not consistent with gravitational deflection: First, PDMS nanoslits would collapse even if they were placed with nanoslit grooves facing upward under the glass substrate. Second, PDMS nanoslits would collapse simultaneously if gravitation deflection were a primary reason for roof collapse however, the roof collapse is apparently a cooperative effect whereby the roof segments sequentially bind to the bottom substrate in a zipper-like fashion instead of simultaneous collapsing. We do not fully understand how the initial contact of PDMS nanoslits on the substrate starts, but we have observed that a small portion of initial adhesion spreads out resulting in roof collapse. Instead of gravitation sagging, the adhesion between a glass substrate and a roof of PDMS nanoslits is accepted as the actual mechanism of roof collapse.<sup>18,24</sup> A theoretical model recently developed is able to predict the stability as

$$\frac{64}{\pi^2} \frac{\gamma}{E'} \frac{w}{h^2} \ln \left[ \sec \left( \frac{\pi}{4} \right) \right] < 0.83 \quad (1)$$

where  $\gamma$  is the work of adhesion (50 mJ/m<sup>2</sup> in the case of PDMS on silicon wafer),  $E'$  is plane-strain elastic modulus of PDMS (3.73 MPa),  $h$  is height, and  $w$  is the width and spacing of nanoslits (Fig. 1).<sup>18</sup> From the equation 1, we can define the stability of nanoslits by rearranging the equation like

$$\text{Stability} \sim \frac{h^2 E'}{w \gamma} \quad (2)$$

Equation 2 shows the stability of nanoslits depending on the height, width, elastic modulus, and adhesion energy. Based on this relationship, we have experimentally searched stable PDMS nanoslits by varying widths and heights for preventing roof collapse. We have fabricated 30 different dimensions as listed in Table 1. The widths of nanoslit are 20  $\mu\text{m}$ , 40  $\mu\text{m}$ , 60  $\mu\text{m}$ , 80  $\mu\text{m}$ , and 100  $\mu\text{m}$ . The heights are 2.2  $\mu\text{m}$ , 1.1  $\mu\text{m}$ , 0.49  $\mu\text{m}$ , 0.34  $\mu\text{m}$ , 0.23  $\mu\text{m}$ , and 0.13  $\mu\text{m}$ , controlled by mixing ratios of a photoresist (AZ-GXR) and a thinner (ZA1500). As shown in Table 1, microslits of 2.15  $\mu\text{m}$  and 1.13  $\mu\text{m}$  are always stable regardless of slit width. Nanoslits of 490 nm and 340 nm show increased stability with decreased widths. However, nanoslits of 130 nm and 230 nm completely collapse and disappear on the flat glass surface.

In addition to widths and heights, equation 2 shows the dependence of stability on adhesion energy and elastic modulus. There are a number of approaches to reduce adhesion energy and increase elastic modulus. For example, we have noticed that longer curing time increases the elastic modulus with increased stiffness. The adhesion energy of PDMS on glass surface is weaker than one of PDMS on silicon wafer. Therefore, decreasing adhesion energy and increasing elastic modulus can be a key approach to achieve stable PDMS nanoslits without roof collapse.

**Plasma Treatment.** PDMS surface conforms and binds onto the glass surface very tightly with van der Waals interaction. The natural hydrophobic property of PDMS surface contributes to tight binding on the glass surface. However, we have observed that a hydrophilic PDMS surface binds the glass surface less strongly than a hydrophobic PDMS surface does;

**Table 1.** Percentage of stable nanoslit structures with various widths and heights. The data were obtained from a PDMS device that is about 12~15 mm wide 5 mm long with alternative channel and gap patterns of the same width. The percentages of stable nanoslits were obtained by counting the number of stable nanoslits out of total number of nanoslits. If nanoslits partially collapse, the length of stable portions were measured. Before counting stable nanoslits, one minute is awaited after PDMS mounting

| Height(m) | Surface Property              | Width             |                  |                  |                  |                  |
|-----------|-------------------------------|-------------------|------------------|------------------|------------------|------------------|
|           |                               | 100 $\mu\text{m}$ | 80 $\mu\text{m}$ | 60 $\mu\text{m}$ | 40 $\mu\text{m}$ | 20 $\mu\text{m}$ |
| 2.15      | All                           | 100%              | 100%             | 100%             | 100%             | 100%             |
| 1.13      | All                           | 100%              | 100%             | 100%             | 100%             | 100%             |
| 0.49      | Hydrophobic                   | 3%                | 7%               | 20%              | 92%              | 100%             |
|           | Hydrophilic                   | 8%                | 20%              | 50%              | 99%              | 100%             |
|           | Glass supported & hydrophilic | 10%               | 50%              | 67%              | 100%             | 100%             |
| 0.34      | Hydrophobic                   | 0%                | 0%               | 0%               | 89%              | 90%              |
|           | Hydrophilic                   | 0%                | 0%               | 3%               | 90%              | 90%              |
|           | Glass supported & hydrophilic | 9%                | 22%              | 35%              | 100%             | 100%             |
| 0.23      | All                           | 0%                | 0%               | 0%               | 0%               | 0%               |
| 0.13      | All                           | 0%                | 0%               | 0%               | 0%               | 0%               |

hydrophilization can be a way to reduce adhesion energy. Thus, we have prepared the hydrophilic PDMS surfaces by treating in air plasma and stored them in water (see Experimental section). The plasma treatment increases the stability by reducing adhesion energy as expected from Eq. 2 (Table 1). For example, only 20% hydrophobic nanoslits of  $60\ \mu\text{m} \times 490\ \text{nm}$  remain stable but 50% hydrophilic nanoslits are stable with the same dimensions. Though plasma treatment generally increases the stability a little bit, this change is not enough to prevent roof collapse of PDMS nanoslits.

**Glass Support.** The stability of PDMS nanoslit is dependent on the elastic modulus as well as adhesion energy. In order to increase the elastic modulus or stiffness of PDMS device, we have designed a method to fix the PDMS device not to deform by attaching a piece of rigid slide glass (1 mm thick) on the other side as shown in Fig. 2B. A basic assumption is that the whole body of a PDMS nanoslit device should deform for the roof collapse as illustrated in Fig. 2A. Therefore if the other side of PDMS device is fixed by a rigid substrate, the stability of PDMS nanoslits would increase because they are no longer flexible to deform. Our assumption is somewhat valid for the case of  $60\ \mu\text{m} \times 340\ \text{nm}$  nanoslits showing that PDMS nanoslit

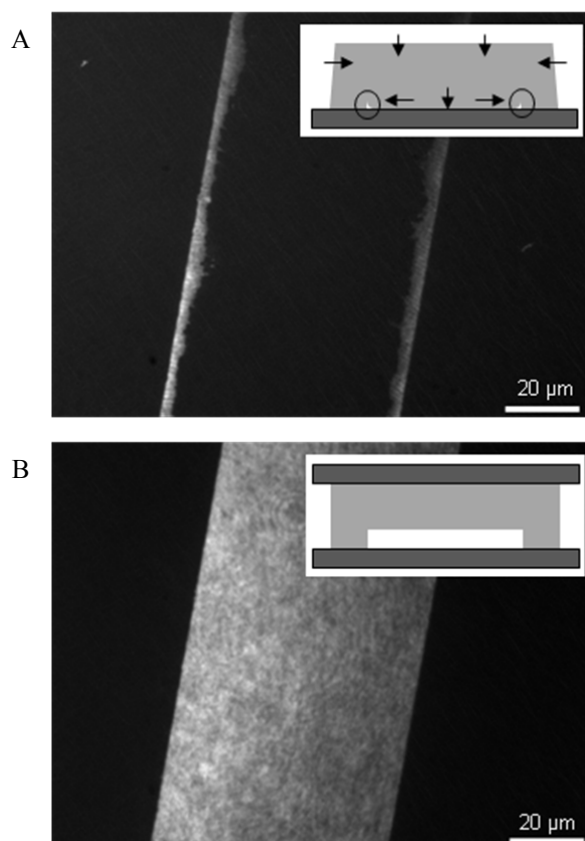


**Figure 2. Glass support.** (A) Roof collapsed nanoslits ( $60\ \mu\text{m} \times 340\ \text{nm}$ ). The illustration in the inset depicts the deformation of PDMS device in the case of roof collapse. Nanoslits are collapsed except gutters formed at the both ends of nanoslits. (B) Glass supported stable PDMS nanoslit ( $60\ \mu\text{m} \times 340\ \text{nm}$ ). The inset illustrates the mechanism of preventing deformation and roof collapsing. In order to visualize nanoslits, the device is filled with black ink which gives off fluorescence excited by 488 nm laser light. Scale bar 20  $\mu\text{m}$ .

with glass support (Fig. 2B) is more stable in one without glass support (Fig. 2A). Even though the idea of glass support improves nanoslits stability for some of 340 nm high channels (Table 1), this approach is not still effective enough to prevent roof collapse for nanoslits of 130 nm and 230 nm.

**Water Filling.** Although plasma treatment and glass support are not enough to make stable PDMS nanoslits, they definitely contribute to the increase of stability. Also we have observed an interesting phenomenon that a plasma-treated and glass-supported nanoslit survives for a few seconds and collapse. This observation gives us a clue that there may be a way to extend this survival period with interrupting roof collapse. One of our hypotheses is that nanoslits would be more stable if the nanoslits are filled with water instead of air; however, it is not easy to fill nanoslits with water before roof collapse starts. We have developed a new way to mount a PDMS nanoslit device on a slightly bent glass and fill water into the gap as illustrated in Fig. 3A (see Experimental section). Then the force for bending a cover glass is removed and PDMS nanoslits are formed by excluding water from the area touching the bottom surface in a couple of minute. Fig. 3B shows an image of  $100\ \mu\text{m} \times 130\ \text{nm}$  nanoslit formed by water filling approach. In this experiment, the black ink is loaded after PDMS nanoslits are formed with water filling. The black fountain pen ink gives bright red fluorescence excited by 488 nm laser light (Fig. 3B). We do not fully understand how prefilled water prevents roof collapse. A plausible hypothesis is that water molecules hydrate PDMS surface which create an energy barrier for adhesion because water molecules should be removed from PDMS and glass surfaces for the roof collapse. Water filling seems to play a key role in preventing roof collapse of nanoslits, but plasma treatment and glass support are indispensable to make stable PDMS nanoslits since we have noticed that nanoslits collapse without plasma treatment and glass support. Therefore, the stable PDMS nanoslits are the result of combination of plasma treatment, glass support, and water filling.

**DNA in Nanoslit.** Nanoslits have been utilized for the study of statics and dynamics of confined single DNA molecules though nanoslits in previous studies are made of hard materials

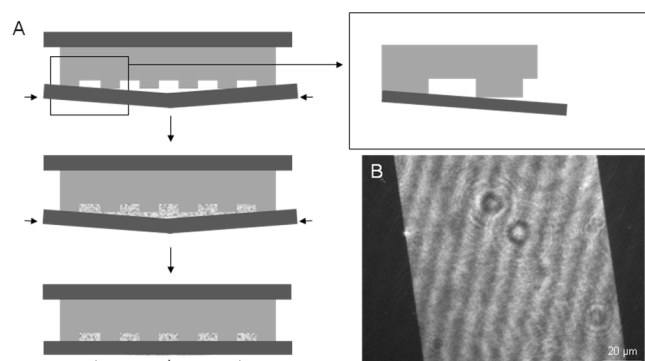


**Figure 3. Water Filling.** (A) Schematics of preparing 100  $\mu\text{m}$  wide 130 nm high nanoslits, which are filled with water. (B) Fluorescent micrograph of  $100\ \mu\text{m} \times 130\ \text{nm}$  nanoslits filled with black ink. Black ink gives off fluorescence and laser diffraction pattern are shown in this picture. Diffraction patterns in the nanoslit are caused by optical laser diffraction. Scale bar is 20  $\mu\text{m}$ .

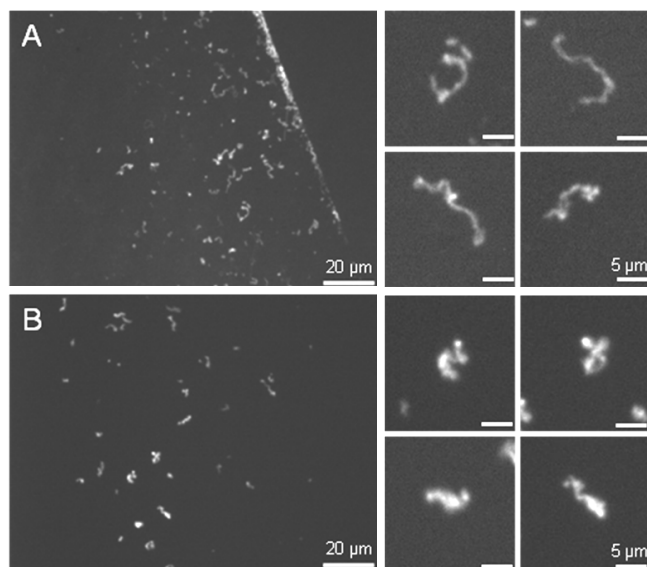


**Figure 4.** DNA molecules (T4 DNA; 166 kb,  $R_g$  1.8  $\mu\text{m}$ ) confined in PDMS nanoslits. (A) DNA molecules in 130 nm  $\times$  80  $\mu\text{m}$  nanoslits. (B) Comparison of DNA molecules in 1.13  $\mu\text{m}$   $\times$  80  $\mu\text{m}$  microslits. Gallery of micrographs of individual molecules (right) are selected and magnified from the large picture (left). Scale bars for large pictures (left) are 20  $\mu\text{m}$  and scale bars for molecules (right) are 5  $\mu\text{m}$ .

such as quartz and fused-silica. DNA molecules are sphere-shaped random coils with radius of gyration ( $R_g$ ) in free solution, but they are stretched widely confined in nanoslits particularly when the height of nanoslit is significantly lower than  $R_g$  and on the order of DNA's persistence length. In this paper, we demonstrate the feasibility of PDMS nanoslits for this study by using T4 DNA (166 kb)  $R_g$  of YOYO-1 stained DNA is 1.8  $\mu\text{m}$  and the persistence length is about 100 nm in a solution of 0.03 $\times$ TE (300  $\mu\text{M}$  Tris and 30  $\mu\text{M}$  EDTA) and 4%  $\beta$ -mercaptoethanol. Fig. 4 shows typical fluorescent images presenting several individual DNA molecules confined and widely stretched in nanoslits (130 nm high 80  $\mu\text{m}$  wide) than DNA molecules in microslit (1.13  $\mu\text{m}$  high 80  $\mu\text{m}$  wide). As expected, DNA molecules in 130 nm nanoslits show a confinement effect.

### Conclusion

We present a new and easy approach for the formation of stable PDMS nanoslits without roof collapse. Our approach obviates the need for technologically demanding nanofabrication of hard materials. We improve the stability of PDMS nanoslits with plasma-treatment, glass support, and water filling. Finally, we successfully make stable 100  $\mu\text{m}$  wide but 130 nm high PDMS nanoslits. Also, we demonstrate the confinement effect of single DNA molecules in PDMS nanoslits. We believe that a new method for building PDMS nanoslits may lay the basis for novel nanofabrication platforms and supplant

hard material nanofabrication due to their ease of procedures. The ability of formation of PDMS nanoslits ensures its use in an increasingly wider range of biochemical and bioanalytical applications.

**Acknowledgments.** This work was supported by the Sogang University Research Grant No. 200810019.01, and also supported by Basic Science Research Program through the National Research Foundation of Korea (NRF) funded by the Ministry of Education, Science and Technology (2009-0078034 and 2009-0069651).

### References

- Manz, A.; Miyahara, Y.; Miura, J.; Watanabe, Y.; Miyagi, H.; Sato, K. *Sens. Act. B Chem.* **1990**, *1*, 249.
- Whitesides, G. M. *Nature* **2006**, *442*, 368.
- Harrison, D. J.; Fluri, K.; Seiler, K.; Fan, Z. H.; Effenhauser, C. S.; Manz, A. *Science* **1993**, *261*, 895.
- Craighead, H. G. *Science* **2000**, *290*, 1532.
- El-Ali, J.; Sorger, P. K.; Jensen, K. F. *Nature* **2006**, *442*, 403.
- Xia, Y. N.; Whitesides, G. M. *Ann. Rev. Mat. Sci.* **1998**, *28*, 153.
- Whitesides, G. M.; Ostuni, E.; Takayama, S.; Jiang, X. Y.; Ingber, D. E. *Ann. Rev. Biomed. Eng.* **2001**, *3*, 335.
- Jo, K.; Dhingra, D. M.; Odijk, T.; de Pablo, J. J.; Graham, M. D.; Runnheim, R.; Forrest, D.; Schwartz, D. C. *Proc. Natl. Acad. Sci. U. S. A.* **2007**, *104*, 2673.
- Zhang, C.; Zhang, F.; van Kan, J. A.; van der Maarel, J. R. C. *J. Chem. Phys.* **2008**, 128.
- Cao, H.; Yu, Z. N.; Wang, J.; Tegenfeldt, J. O.; Austin, R. H.; Chen, E.; Wu, W.; Chou, S. Y. *App. Phys. Lett.* **2002**, *81*, 174.
- Reisner, W.; Beech, J. P.; Larsen, N. B.; Flyvbjerg, H.; Kristensen, A.; Tegenfeldt, J. O. *Phys. Rev. Lett.* **2007**, 99.
- Tegenfeldt, J. O.; Prinz, C.; Cao, H.; Chou, S.; Reisner, W. W.; Riehn, R.; Wang, Y. M.; Cox, E. C.; Sturm, J. C.; Silberzan, P.; Austin, R. H. *Proc. Natl. Acad. Sci. U. S. A.* **2004**, *101*, 10979.
- Effenhauser, C. S.; Bruin, G. J. M.; Paulus, A.; Ehrat, M. *Anal. Chem.* **1997**, *69*, 3451.
- Strychalski, E. A.; Levy, S. L.; Craighead, H. G. *Macromolecules* **2008**, *41*, 7716.
- Hsieh, C. C.; Balducci, A.; Doyle, P. S. *Nano Lett.* **2008**, *8*, 1683.
- Balducci, A. G.; Tang, J.; Doyle, P. S. *Macromolecules* **2008**, *41*, 9914.
- Hui, C. Y.; Jagota, A.; Lin, Y. Y.; Kramer, E. J. *Langmuir* **2002**, *18*, 1394.
- Huang, Y. G. Y.; Zhou, W. X.; Hsia, K. J.; Menard, E.; Park, J. U.; Rogers, J. A.; Alleyne, A. G. *Langmuir* **2005**, *21*, 8058.
- Zhou, W.; Huang, Y.; Menard, E.; Aluru, N. R.; Rogers, J. A.; Alleyne, A. G. *App. Phys. Lett.* **2005**, 87.
- Decre, M. M. J.; Timmermans, P. H. M.; van der Sluis, O.; Schroeders, R. *Langmuir* **2005**, *21*, 7971.
- Duffy, D. C.; McDonald, J. C.; Schueller, O. J. A.; Whitesides, G. M. *Anal. Chem.* **1998**, *70*, 4974.
- Dimalanta, E. T.; Lim, A.; Runnheim, R.; Lamers, C.; Churas, C.; Forrest, D. K.; de Pablo, J. J.; Graham, M. D.; Coppersmith, S. N.; Goldstein, S.; Schwartz, D. C. *Anal. Chem.* **2004**, *76*, 5293.
- Sharp, K. G.; Blackman, G. S.; Glassmaker, N. J.; Jagota, A.; Hui, C. Y. *Langmuir* **2004**, *20*, 6430.
- Hsia, K. J.; Huang, Y.; Menard, E.; Park, J. U.; Zhou, W.; Rogers, J.; Fulton, J. M. *App. Phys. Lett.* **2005**, *86*, 154106.